Severe Preeclampsia-Related Changes in Gene Expression at the Maternal-Fetal Interface Include Sialic Acid-Binding Immunoglobulin-Like Lectin-6 and Pappalysin-2

Virginia D. Winn, Matthew Gormley, Agnes C. Paquet, Kasper Kjaer-Sorensen, Anita Kramer, Kristen K. Rumer, Ronit Haimov-Kochman, Ru-Fang Yeh, Michael T. Overgaard, Ajit Varki, Claus Oxvig, and Susan J. Fisher

Departments of Obstetrics, Gynecology, and Reproductive Sciences (V.D.W., M.G., R.H.-K.), Cell and Tissue Biology (R.H.-K., S.J.F.), Medicine Lung Biology Center (A.C.P., R.-F.Y.), and Anatomy and Pharmaceutical Chemistry (S.J.F.), University of California, San Francisco, San Francisco, California 94143; Department of Obstetrics and Gynecology (V.D.W., A.K., K.K.R.), University of Colorado Denver, Aurora, Colorado 80045; Department of Molecular and Cellular Medicine (A.V.), University of California, San Diego, San Diego, California 92093; and Department of Molecular Biology (K.K.-S., M.T.O., C.O.), University of Aarhus, DK-8000 Aarhus C, Denmark

Preeclampsia (PE), which affects 4–8% of human pregnancies, causes significant maternal and neonatal morbidity and mortality. Within the basal plate, placental cytotrophoblasts (CTBs) of fetal origin invade the uterus and extensively remodel the maternal vasculature. In PE, CTB invasion is often shallow, and vascular remodeling is rudimentary. To better understand possible causes, we conducted a global analysis of gene expression at the maternal-fetal interface in placental samples from women with PE (n = 12; 24–36 wk) *vs.* samples from women who delivered due to preterm labor with no evidence of infection (n = 11; 24–36 wk), a condition that our previous work showed is associated with normal CTB invasion. Using the HG-U133A&B Affymetrix GeneChip platform, and statistical significance set at log odds-ratio of B >0, 55 genes were differentially expressed in PE. They encoded proteins previously associated with PE [*e.g.* Flt-1 (vascular endothelial growth factor receptor-1), leptin, CRH, and inhibin] and novel molecules [*e.g.* sialic acid binding Ig-like lectin 6 (Siglec-6), a potential leptin receptor, and pappalysin-2 (PAPP-A2), a protease that cleaves IGF-binding proteins]. We used quantitative PCR to validate the expression patterns of a subset of the genes. At the protein level, we confirmed PE-related changes in the expression of Siglec-6 and PAPP-A2, which localized to invasive CTBs and syncytiotrophoblasts. Notably, Siglec-6 placental expression is uniquely human, as is spontaneous PE. The functional significance of these novel observations may provide new insights into the pathogenesis of PE, and assaying the circulating levels of these proteins could have clinical utility for predicting and/or diagnosing PE. **(*Endocrinology* 150: 452–462, 2009)**

Preeclampsia (PE), a pregnancy complication, is manifested by the onset of hypertension and proteinuria in the second half of pregnancy. PE is relatively common (4–8% of pregnancies), with potentially deadly consequences for the mother and/or her offspring. Currently, the only definitive treatment for this condition is delivery of the placenta, and therefore the infant, accounting for 15% of all preterm births in the United States. Despite decades of research, a full understanding of the pathogenesis of PE remains elusive, hampering the development of better predictive tests, methods of diagnosis, and therapeutic interventions. Nevertheless, it is clear that the placenta plays a central role; the signs of PE can occur in molar pregnancies, which lack a fetus, and the disease resolves once the placenta is delivered. Interestingly, spontaneous PE does not occur in other animals, including nonhuman primates.

Formation of the human placenta entails differentiation of its

ISSN Print 0013-7227 ISSN Online 1945-7170
Printed in U.S.A.

doi: 10.1210/en.2008-0990 Received July 2, 2008. Accepted September 15, 2008.
First Published Online September 25, 2008

Abbreviations: CTB, Cytotrophoblast; IGFBP, IGF-binding protein; PAPP-A2, pappalysin-2; PE, preeclampsia; PTL, preterm labor; PVDF, polyvinylidene difluoride; Q-PCR, quantitative PCR; Siglec-6, sialic acid binding Ig-like lectin 6; SOCS, suppressor of cytokine signaling; STB, syncytiotrophoblast; VEGFR, vascular endothelial growth factor receptor.

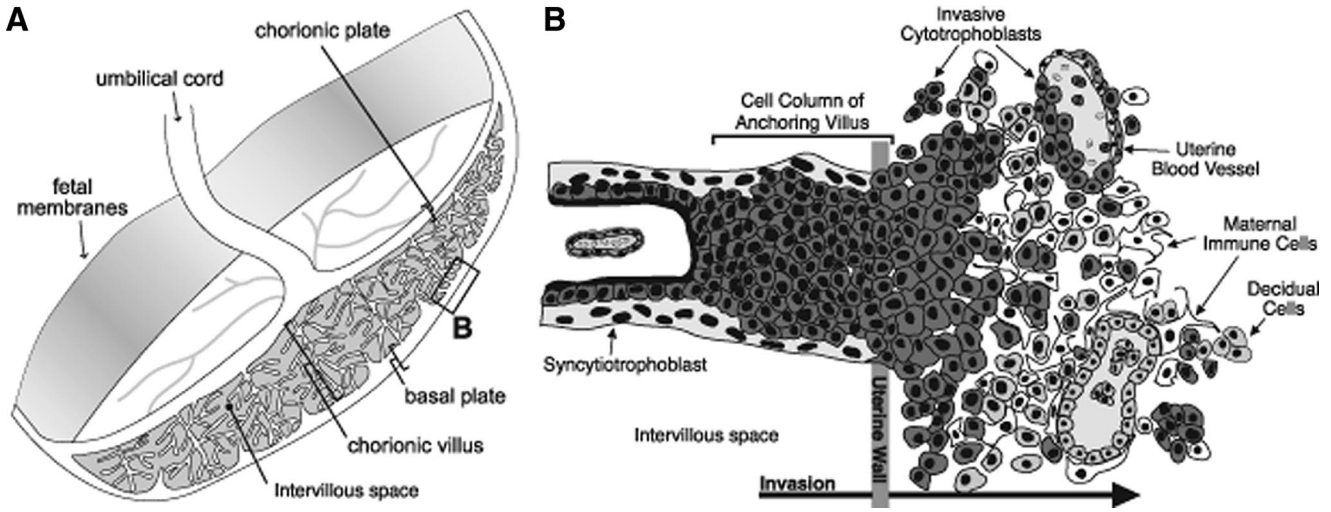

FIG. 1. Diagram of the human maternal-fetal interface. A, Representation of the human placenta after delivery. The placental surface that was adjacent to the uterine wall is termed the basal plate. The *boxed area* denotes the region biopsied for these studies. B, View of the basal plate at the cellular level. This chimeric region of the placenta is composed of both maternal and fetal components: extravillous (invasive) cytotrophoblasts (*dark gray*), decidual cells (*light gray*), remodeled vasculature (both invasive CTBs and maternal endothelium), and maternal immune cells (*white*). [Reproduced with permission from V. D. Winn *et al.*: Endocrinology 148:1059, 2007 (17). ©The Endocrine Society.]

specialized progenitor cells, termed cytotrophoblasts (CTBs), a process that establishes the architecture of the placenta and the maternal-fetal interface or basal plate (Fig. 1). During CTB differentiation, progenitors assume one of two fates. In floating villi, they fuse to form multinucleate syncytiotrophoblasts (STBs), whose primary functions are transport and hormone production. In anchoring villi, mononuclear CTBs acquire tumor-like properties that enable them to invade the decidua, the endometrium of pregnancy, and the adjacent third of the myometrium (interstitial invasion). They also breach the small uterine vessels they encounter, completely replacing the resident maternal endothelial lining and intercalating within the muscular walls, a process that involves nearly the entire intrauterine course of arterioles, but only the termini of veins (endovascular invasion). As a result, high-resistance spiral arterioles are transformed into low-resistance, high-capacitance vessels that divert uterine blood flow to the floating villi. This process is most active during 10–20 wk of gestation, before the onset of the clinical symptoms of PE.

During the last several years, a clearer picture of the pathogenesis of PE has begun to emerge. A two-stage model has been proposed in which the initiating event, poor placentation, is thought to occur early in gestation (1). This concept is supported by several studies that document the association between reduced blood flow to the placenta before 20 wk gestation, as determined by color Doppler ultrasound evaluation of terine arterial blood flow, and a greatly increased risk of developing PE (2, 3). Anatomic examination shows that the specific area of the placenta most affected by this syndrome is the basal plate, the site of CTB invasion. Interstitial CTB invasion is often shallow, and endovascular invasion does not proceed beyond the terminal portions of the spiral arterioles. Thus, the maternal vessels do not undergo the complete spectrum of physiological changes that normally occur (*e.g.* loss of endothelial lining and musculoelastic tissue); the mean external diameter of the myometrial vessels is less than half that of equivalent vessels from uncomplicated pregnancies (4–6). In addition, fewer vessels show evidence of CTB invasion (7). Thus, their architecture precludes an adequate response to gestation-related fetal demands for increased blood flow.

The second stage of PE is thought to be the maternal response to abnormal placentation. Systemic endothelial dysfunction appears to be an important common denominator (1, 8, 9). Recent data point to an imbalance in circulating factors with angiogenic/vasculogenic functions, such as soluble vascular endothelial growth factor receptor-1 (VEGFR-1, sFlt-1), placental growth factor, and the TGF-β receptor endoglin (10–16).

The studies reported here employed an unbiased approach that required no previous knowledge of the molecules involved to achieve a better understanding of PE pathogenesis. Specifically, we used a microarray platform to evaluate gene expression patterns at a global level in the basal plate region, the area of CTB invasion, of affected individuals compared with control subjects who were matched for gestational age at the time of delivery. The importance of controlling for gestational age is illustrated by our recent work on gene expression changes at the maternal-fetal interface that revealed dramatic differences between migestation and term (17). In this regard, we exploited our recent observation that preterm labor (PTL) without signs of inflammation is associated with normal CTB differentiation/invasion. We did this by using basal plate samples collected from patients who delivered due to this pregnancy complication as gestation-matched controls (18). The results of the current study revealed 55 differentially expressed genes, of which the majority were not known to be dysregulated in severe PE. The results of this work highlight the complex pathophysiology of this condition and the many pathways it impacts.

Materials and Methods

Tissue collection

The University of California, San Francisco (UCSF), Committee on Human Research approved this study. Informed consent was obtained from each parturient tissue donor before delivery. Basal plate biopsy specimens of the maternal-fetal interface were collected from individuals who developed severe PE or PTL without signs of infection. Pregnancies complicated by multiple gestations, fetal anomalies, premature rupture of the membranes, infection, diabetes, or other autoimmune diseases were excluded. Gestational age was determined by using standard dating criteria (19). The basal plate was dissected and processed from the placenta proper as previously described (17). All samples were processed within 2 h of delivery.

Total RNA extraction

RNA was isolated from snap-frozen basal plate specimens using a modified Trizol method as previously described (20). Aliquots were evaluated by using the Agilent RNA 6000 Nano LabChip kit (Agilent Technologies, Santa Clara, CA) on an Agilent Bioanalyzer 2100 system. Capillary electrophoresis data in commaseparated value files were analyzed by using the Degradometer version 1.41 software (available at http://www.dnaarrays.org) (21). Only RNA with a degradation factor of less than 11 was used in subsequent microarray experiments.

Microarray hybridization

The microarray platform was the high-density HG-U133A and HG-U133B GeneChips (Affymetrix, Santa Clara, CA). Sample processing and hybridization was accomplished by using the protocols devised by the UCSF Gladstone (National Heart, Lung, and Blood Institute) Genomics Core Facility (http://www.gladstone.ucsf.edu/gladstone/php/section) as previously described (17). Samples from individual basal plates were analyzed separately. Specifically, the HG-U133A and HG-U133B Affymetrix GeneChips were each hybridized with 15 μg cRNA and then washed, stained, and imaged at the Gladstone Genomics Core Facility by using standard Affymetrix protocols. Data files were deposited in the GEO (Gene Expression Omnibus) data repository (accession no. pending).

Data analysis

The raw image data were analyzed by using GeneChip Expression Analysis software (Affymetrix) to produce perfect match and mismatch values. Subsequently, quality control, preprocessing, and linear modeling were performed using Bioconductor (22), an open source and open development software project based on the R statistical package (http://www.r-project.org). Initial hybridization quality was assessed using the Bioconductor package affyPLM, and slight variations in quality were compensated for during the preprocessing stage, which was performed in two steps. First, we used a Probe Level robust linear model (23) to obtain separate normalized log intensities for each chip (*i.e.* background subtraction, quantile normalization, and probe set summarization). Second, we applied a global median normalization at the probe set level to all A and B GeneChips (n = 46) and then combined these data into a matrix of $\log_2$-based gene expression measures, in which columns corresponded to different cRNA samples, and rows corresponded to the different probe sets.

Estimated log ratios (M value) between cases and controls were determined by using the limma software package in R (24). Then differentially expressed genes were selected by statistical analysis of LOD ratios, and B >0 was set as significant. The results showed that the expression of 55 genes (71 probe sets) was significantly modulated. Then the normalized intensity values for this data set were centered to the median intensity value for each probe set, after which the probe sets were ranked according to their M values (representing fold change) and depicted as a gene expression color map. Evaluation of these filtered probes in the context of both clinical and experimental variables was performed to assess confounding factors.

Quantitative PCR

Reverse transcription of RNA (total) samples isolated from basal plate biopsies was carried out as previously described (17). All templates were amplified with Assay-on-Demand kits (Applied Biosystems, Foster City, CA) or primer/probe sets designed by the UCSF Biomolecular Research Center (see supplemental Table SI, published as supplemental data on The Endocrine Society's Journals Online web site at http://endo.endojournals.org). Quantitative PCR (Q-PCR) was carried out as previously described (17). Negative control RNA samples were not reverse transcribed or lacked template inputs. Relative quantification was determined by using the standard curve method (see Applied Biosystems User Bulletin no. 2; http://www3.appliedbiosystems.com). In preliminary experiments, we investigated the utility of 11 potential targets as endogenous controls (endogenous control plate; Applied Biosystems). The results showed that the 18S rRNA did not vary with gestational age or disease state. Accordingly, the levels of this transcript were used to obtain normalized values for the target amplicons. A 24-wk PTL sample, the earliest gestational age included in our analysis, was used as the calibrator for the relative quantification using the standard curve method. Results are reported as the relative fold mRNA levels $\pm$ SD for each basal plate specimen. The mean values of the PE and PTL samples were compared using a two-tailed Student's *t* test ($P < 0.05$).

Sialic acid binding Ig-like lectin 6 (Siglec-6) immunohistochemistry

Serial sections (5 μm) from formalin-fixed tissues were deparaffinized and rehydrated. Staining was performed as previously published (25). The tissue sections were incubated overnight at 4 C with one of the primary antibodies [anti-Siglec-6 (26), 1:25, or anti-cytokeratin-7 (anti-CK-7) clone OV-TL 12/30 (Dako, Carpinteria, CA), diluted 1:50 in DakoCytomatin antibody diluent (Dako)]. Negative control tissue sections were incubated without primary antibody. Visualization was achieved by incubation with diaminobenzidine for 2 min following the manufacturer's instructions (Vector Laboratories, Burlingame, CA), and nuclei were counterstained with hematoxylin QS (Vector Laboratories). The tissue sections were imaged by using a Nikon eclipse 80i microscope and photographed with a Q-imaging Retiga 2000R digital camera.

For immunofluorescence staining, frozen sections (5 μm) from OCT-embedded tissues were washed in PBS, and nonspecific reactivity was blocked by incubating with 3% BSA (wt/vol), 0.1% Triton X-100 (vol/vol), and 0.5% Tween 20 (vol/vol) in PBS for 30 min. Then sections were incubated with anti-Siglec-6 (1:100 in blocking buffer) for 1 h and washed in PBS. Negative controls were incubated without the primary antibody. Sections were then exposed to anti-CK-7 [clone 7D3 (27), 1:100] for 1 h and washed in PBS as described above. The sections were then incubated with Alexa Fluor 594-conjugated goat antimouse IgG (1:1000; Molecular Probes Inc., Eugene, OR) and fluorescein isothiocyanate-labeled donkey antirat IgG (1:200; Jackson ImmunoResearch Laboratories, West Grove, PA) antibodies for 30 min and washed in PBS. Tissue sections were mounted in Vectashield containing 4′,6-diamidino-2-phenylindole (Vector Laboratories), which allowed visualization of the nuclei. Imaging was done using a Leica DM 5000B fluorescence microscope equipped with a Leica DFC 350FX digital camera (Leica Microsystems, Bannockburn, IL; and Leica-Camera, Solms, Germany).

Generation of antihuman pappalysin-2 (PAPP-A2) polyclonal serum

A fragment encoding Ser-234 to Gln-495 of PAPP-A2 was amplified by PCR using the plasmid pPA2 as the template (28). The forward primer was 5′-CGATAGATCT**ATCGAGGGTAGG**AGTCCACCG-GAGGAAAGCAAC-3′ (a *Bgl*II site is *underlined*, and a factor Xa recognition site is shown in *bold*). The reverse primer was 5′-CGATA-AGCTT**TCA**CTGCAAAGGCGACAGAATCTC-3′ (a *Hin*dIII site is

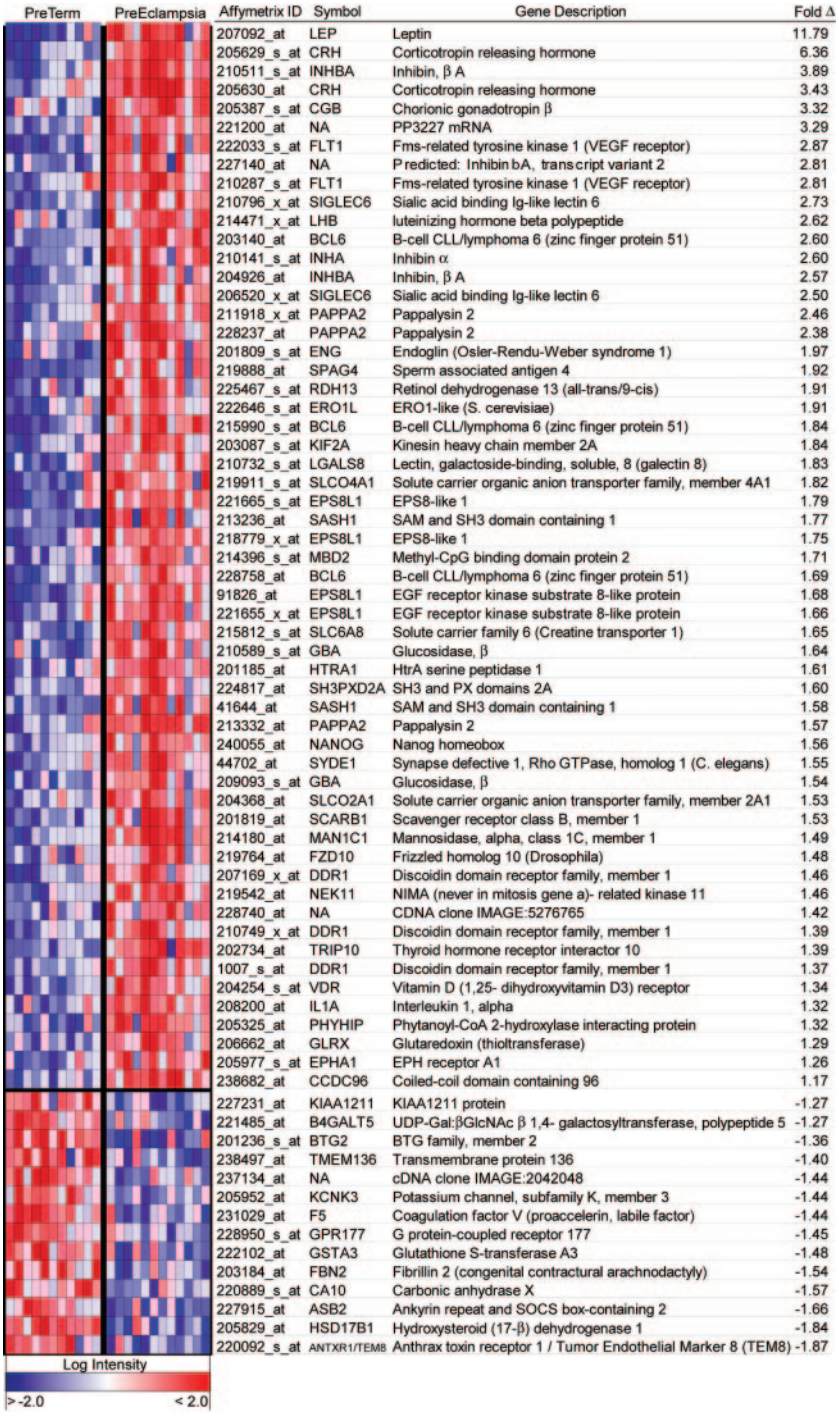

Affymetrix ID	Symbol	Gene Description	Fold Δ
207092_at	LEP	Leptin	11.79
205629_s_at	CRH	Corticotropin releasing hormone	6.36
210511_s_at	INHBA	Inhibin, β A	3.89
205630_at	CRH	Corticotropin releasing hormone	3.43
205387_s_at	CGB	Chorionic gonadotropin β	3.32
221200_at	NA	PP3227 mRNA	3.29
222033_s_at	FLT1	Fms-related tyrosine kinase 1 (VEGF receptor)	2.87
227140_at	NA	Predicted: Inhibin bA, transcript variant 2	2.81
210287_s_at	FLT1	Fms-related tyrosine kinase 1 (VEGF receptor)	2.81
210796_x_at	SIGLEC6	Sialic acid binding Ig-like lectin 6	2.73
214471_x_at	LHB	luteinizing hormone beta polypeptide	2.62
203140_at	BCL6	B-cell CLL/lymphoma 6 (zinc finger protein 51)	2.60
210141_s_at	INHA	Inhibin α	2.60
204926_at	INHBA	Inhibin, β A	2.57
206520_x_at	SIGLEC6	Sialic acid binding Ig-like lectin 6	2.50
211918_x_at	PAPPA2	Pappalysin 2	2.46
228237_at	PAPPA2	Pappalysin 2	2.38
201809_s_at	ENG	Endoglin (Osler-Rendu-Weber syndrome 1)	1.97
219888_at	SPAG4	Sperm associated antigen 4	1.92
225467_s_at	RDH13	Retinol dehydrogenase 13 (all-trans/9-cis)	1.91
222646_s_at	ERO1L	ERO1-like (S. cerevisiae)	1.91
215990_s_at	BCL6	B-cell CLL/lymphoma 6 (zinc finger protein 51)	1.84
203087_s_at	KIF2A	Kinesin heavy chain member 2A	1.84
210732_s_at	LGALS8	Lectin, galactoside-binding, soluble, 8 (galectin 8)	1.83
219911_s_at	SLCO4A1	Solute carrier organic anion transporter family, member 4A1	1.82
221665_s_at	EPS8L1	EPS8-like 1	1.79
213236_at	SASH1	SAM and SH3 domain containing 1	1.77
218779_x_at	EPS8L1	EPS8-like 1	1.75
214396_s_at	MBD2	Methyl-CpG binding domain protein 2	1.71
228758_at	BCL6	B-cell CLL/lymphoma 6 (zinc finger protein 51)	1.69
91826_at	EPS8L1	EGF receptor kinase substrate 8-like protein	1.68
221655_x_at	EPS8L1	EGF receptor kinase substrate 8-like protein	1.66
215812_s_at	SLC6A8	Solute carrier family 6 (Creatine transporter 1)	1.65
210589_s_at	GBA	Glucosidase, β	1.64
201185_at	HTRA1	HtrA serine peptidase 1	1.61
224817_at	SH3PXD2A	SH3 and PX domains 2A	1.60
41644_at	SASH1	SAM and SH3 domain containing 1	1.58
213332_at	PAPPA2	Pappalysin 2	1.57
240055_at	NANOG	Nanog homeobox	1.56
44702_at	SYDE1	Synapse defective 1, Rho GTPase, homolog 1 (C. elegans)	1.55
209093_s_at	GBA	Glucosidase, β	1.54
204368_at	SLCO2A1	Solute carrier organic anion transporter family, member 2A1	1.53
201819_at	SCARB1	Scavenger receptor class B, member 1	1.53
214180_at	MAN1C1	Mannosidase, alpha, class 1C, member 1	1.49
219764_at	FZD10	Frizzled homolog 10 (Drosophila)	1.48
207169_x_at	DDR1	Discoidin domain receptor family, member 1	1.46
219542_at	NEK11	NIMA (never in mitosis gene a)- related kinase 11	1.46
228740_at	NA	CDNA clone IMAGE:5276765	1.42
210749_x_at	DDR1	Discoidin domain receptor family, member 1	1.39
202734_at	TRIP10	Thyroid hormone receptor interactor 10	1.39
1007_s_at	DDR1	Discoidin domain receptor family, member 1	1.37
204254_s_at	VDR	Vitamin D (1,25- dihydroxyvitamin D3) receptor	1.34
208200_at	IL1A	Interleukin 1, alpha	1.32
205325_at	PHYHIP	Phytanoyl-CoA 2-hydroxylase interacting protein	1.32
206662_at	GLRX	Glutaredoxin (thioltransferase)	1.29
205977_s_at	EPHA1	EPH receptor A1	1.26
238682_at	CCDC96	Coiled-coil domain containing 96	1.17
227231_at	KIAA1211	KIAA1211 protein	-1.27
221485_at	B4GALT5	UDP-Gal:βGlcNAc β 1,4- galactosyltransferase, polypeptide 5	-1.27
201236_s_at	BTG2	BTG family, member 2	-1.36
238497_at	TMEM136	Transmembrane protein 136	-1.40
237134_at	NA	cDNA clone IMAGE:2042048	-1.44
205952_at	KCNK3	Potassium channel, subfamily K, member 3	-1.44
231029_at	F5	Coagulation factor V (proaccelerin, labile factor)	-1.44
228950_s_at	GPR177	G protein-coupled receptor 177	-1.45
222102_at	GSTA3	Glutathione S-transferase A3	-1.48
203184_at	FBN2	Fibrillin 2 (congenital contractural arachnodactyly)	-1.54
220889_s_at	CA10	Carbonic anhydrase X	-1.57
227915_at	ASB2	Ankyrin repeat and SOCS box-containing 2	-1.66
205829_at	HSD17B1	Hydroxysteroid (17-β) dehydrogenase 1	-1.84
220092_s_at	ANTXR1/TEM8	Anthrax toxin receptor 1 / Tumor Endothelial Marker 8 (TEM8)	-1.87

FIG. 2. Heat map of differentially expressed genes in basal plate of PE placentas compared with controls. The normalized log intensity values for 71 differentially expressed probe sets were centered to the median value of each probe set and colored on a range of −2.5 to +2.5. *Red* denotes up-regulated expression levels, and *blue* denotes down-regulated expression levels as compared with the median value. *Columns* contain data from a single basal plate specimen, and *rows* correspond to a single probe set. Samples are arranged in order of increasing gestational age from *left* to *right* for each category. *Rows* are ranked by fold change [mean PE value (n = 12) divided by mean PTL value (n = 11)].

underlined, and a stop codon is shown in *bold*). The 821-bp product was digested with *Bgl*II and *Hin*dIII, and cloned into the *Bam*HI/*Hin*dIII sites of the *Escherichia coli* expression vector pT7H6UB (29). The resulting construct, pT7H6UBFX_P2_234–495, encoded a fusion protein with an N-terminal hexa-His tag followed by residues 2–76 of human ubiquitin, a factor Xa recognition site, and residues 234–495 of human PAPP-A2. *E. coli* strain BL21 (DE3), transformed with pT7H6UBFX_P2_234–495, was grown at 37 C to an OD_{600} of approximately 0.8. Expression was induced by the addition of isopropyl-β-D-thiogalactopyranoside to a final concentration of 1 mM. After 4 h at 37 C, the bacteria were harvested by centrifugation, resuspended in 20 mM Tris-HCl, 0.5 M NaCl (pH 8.0) (buffer A), and disrupted by sonication, and the lysate was centrifuged. The pellet containing inclusion bodies was washed three times with buffer A containing (2 M urea and 2% Triton X-100), and then redissolved in buffer A containing 8 M urea, and loaded onto a Ni-NTA column (GE Healthcare, Piscataway, NJ). Bound protein was eluted with buffer A containing 8 M urea and 20 mM EDTA and refolded by rapid dilution into 0.4 M L-arginine, 10 mM Tris-HCl (pH 8.0) (30). After concentration, centrifugation, and dialysis into 20 mM Tris-HCl, 100 mM NaCl (pH 8.0), the fusion protein was cleaved with factor Xa (Sigma Chemical Co., St. Louis, MO) to remove the ubiquitin domain. The recombinant PAPP-A2 domain was purified by ion-exchange chromatography on Q-Sepharose (GE Healthcare). Rabbits were immunized with antigen dissolved in Freund's complete adjuvant (Sigma) essentially as described (31). Freund's incomplete adjuvant (Sigma) was used as the vehicle in subsequent injections. Serum was collected at 6-wk intervals.

Immunoblot analysis

To assess the specificity of the anti-PAPP-A2 sera, reduced recombinant PAPP-A2 (0.1 ng), human term pregnancy serum (1 μl), purified PAPP-A/pro-major basic protein complex (0.1 μg) (32), and reduced recombinant PAPP-A (0.1 μg) (33) were separated on a 7% TA Novex gel under reducing conditions and transferred to a polyvinylidene difluoride (PVDF) membrane. Blocking was performed in 2% Tween 20 for 20 min. The membrane was incubated overnight at 4 C with either anti-PAPP-A2 serum or the preimmune serum (1:10,000 dissolved in blocking buffer). After washing, the membrane was incubated with a secondary antibody (antirabbit IgG Dako P217; 1:4000 dissolved in blocking buffer) for 1 h at room temperature. To evaluate placental expression, 10 μg of a protein lysate prepared in RIPA lysis buffer [50 mM Tris-HCl (pH 7.4), 150 mM NaCl, 0.5% Na deoxycholate (wt/vol), 0.1% sodium dodecyl sulfate (wt/vol), and 1% Nonidet P-40 (vol/vol)] supplemented with 1% protease inhibitor cocktail (Sigma) from basal plate specimens obtained from PE (n = 10) or PTL (n = 9) patients was separated on a 4–20% gradient SDS-PAGE gel and transferred to a PVDF membrane. After blocking nonspecific reactivity by incubating in 5% BSA in Tris-buffered saline with Tween 20 (10 mM Tris base; 150 mM NaCl; and 0.05% Tween 20, pH 8.4) for 1 h at room temperature, the membrane was incubated with anti-PAPP-A2 serum (1:10,000 diluted in blocking buffer) overnight at 4 C, washed with Tris-buffered saline with Tween 20, followed by incubation with antirabbit horseradish peroxidase-conjugated antibody (1:10,000 dissolved in blocking buffer) for 1 h at room temperature. Immunoreactive bands were visualized by using chemiluminescence (Pierce, Rockford, IL) and exposure to XR film (Kodak, Rochester, NY). To evaluate for pro-

tein loading, the PVDF membrane was stripped and incubated with anti-actin antibody (C4, 1:10,000; Sigma) for 1 h at room temperature and then processed as described above. Densitometry was performed using QuantityOne software (Bio-Rad, Hercules, CA).

PAPP-A2 immunohistochemistry

Serial sections (5 μm) were deparaffinized and rehydrated before antigen retrieval in citrate buffer (pH 6.8) for 20 min at 95–100 C. Endogenous peroxidase activity was quenched as described above. Nonspecific reactivity was blocked by incubating the tissue sections with preimmune serum (ABC Elite kits; Vector Laboratories) according to the manufacturer's instructions before overnight exposure at 4 C to a primary antibody dissolved in blocking buffer at the concentrations indicated [anti-PAPP-A2, 1:30,000; anti-PAPP-A (34), 1:50; anti-CK-7, 1:100; and anti-HLA-G, 1:50 (35)]. Binding of the primary antibody was detected by incubating the tissue sections in a solution of the species-appropriate secondary antibodies provided in the ABC Elite kits (Vector Laboratories). Control sections were incubated without primary antibody. Visualization, counterstaining, and imaging were performed as described above.

Results

Using a microarray approach to analyze the basal plate regions of placentas obtained from women who experienced PTL (n = 11) and women whose pregnancies were complicated by PE (n = 12), we identified 55 genes (71 probe sets) that were differentially expressed (Fig. 2). Inclusion criteria for the PTL patients included a singleton pregnancy, no evidence of infection (clinical or histological), absence of premature rupture of membranes, and no significant maternal disease. Approximately one third of the women delivered due to a diagnosis of cervical insufficiency. The PE patients fulfilled the criteria for PE as defined in a 2002 American College of Obstetrics and Gynecology bulletin (36). Clinical characteristics of the two groups are compared in Table 1. The majority of PE patients (10 of 12) experienced labor (with or without a cesarean section). Although more patients with PE (n = 6) than with PTL (n = 2) delivered by cesarean section, *post hoc* statistical analyses of the data showed that the method of delivery was not a confounding factor. The characteristics that defined the PE group are shown in Table 2. Among the most highly up-regulated genes were those that encode molecules whose expression was previously reported to be elevated in PE: leptin, VEGFR-1 (the gene that is alternatively spliced to produce sFlt-1), and CRH. In addition, this analysis revealed more than 40 novel transcripts, which to our knowledge have not previously been reported to be differentially expressed in PE or associated with the pathogenesis of this syndrome.

TABLE 1. Clinical characteristics of study groups

	PTL (n = 11)	PE (n = 12)
Maternal age (yr)	30.2 ± 7.1	30.7 ± 9.1
Gestational age (wk)	31.0 ± 4.6	32.1 ± 3.3
Nulliparous	7 (64%)	9 (75%)
Cesarean section	2 (18%)	6 (50%)
Labored	11 (100%)	10 (83%)

Statistical analysis was by χ^2 test. Differences between the two groups were not significant.

TABLE 2. Characteristics of patients with severe PE (n = 12)

	No. of patients
Severe PE blood pressures	9 (83%)
Severe PE proteinuria	6 (50%)
Severe PE abnormal laboratory results	2 (17%)
Eclampsia	2 (17%)
Superimposed PE	2 (17%)
Fetal abnormality[a]	5 (42%)

The median creatinine was 0.9 (range, 0.5–1.3).

[a] Growth restriction, oligohydramnios, or abnormal Doppler ultrasound.

To rule out the possibility that clinical and/or experimental variables accounted for the observed expression patterns, we searched for possible correlations. We found no association with gestational age, parity, labor, maternal age, or fetal sex. Additional variables that were considered included time between betamethasone injection and delivery, other common medications that are used in these patient populations, mode of delivery, criteria for diagnosing PE, RNA degradation value, and tissue-processing time. Furthermore, we evaluated the level of the CTB-specific molecule CK-7, which is expressed by only trophoblasts, to determine that differences did not simply reflect different ratios of fetal to maternal tissue contribution to the samples. CK-7 levels were not different between the PE and PTL samples or with gestational age.

Next, we used a Q-PCR approach to validate the expression patterns of nine genes. They included those genes whose normal expression patterns are known to be dysregulated in PE, which served as positive controls, and a number of novel molecules over a range of expression. The results of these experiments confirmed the expression patterns observed in the microarray analysis; all were statistically significant except hydroxysteroid (17-β) dehydrogenase 1, which showed the same trend (Fig. 3). For comparison, the microarray data are plotted as insets to the individual bar graphs. In accordance with many published studies that have profiled the expression patterns of individual molecules in PE (37, 38), considerable variation among individual samples was apparent. This may be a reflection of the heterogeneity of the fetal and maternal responses to PE.

To further validate our findings, we performed a more extensive, protein-level analysis of novel molecules with PE-associated alterations in their expression patterns that potentially could play important functions in the pathogenesis of this syndrome. In particular, we focused on Siglec-6, which was originally cloned on the basis of its ability to bind leptin (26). Interestingly, leptin expression, known to be dysregulated in PE (39–44), was also markedly increased in our microarray data set (Fig. 2), but the classical leptin receptors (*e.g.* ObR) were not. By applying an immunohistochemical approach, we showed that Siglec-6 expression was in general more pronounced in the basal plate of PE samples (n = 14) than in the PTL controls (n = 11, Fig. 4A). Additionally, we found that PE was associated with a dramatic increase in STB expression of Siglec-6, particularly earlier in gestation (<33 wk), when there was no immunoreactivity in the PTL samples and clear immunoreactivity in PE.

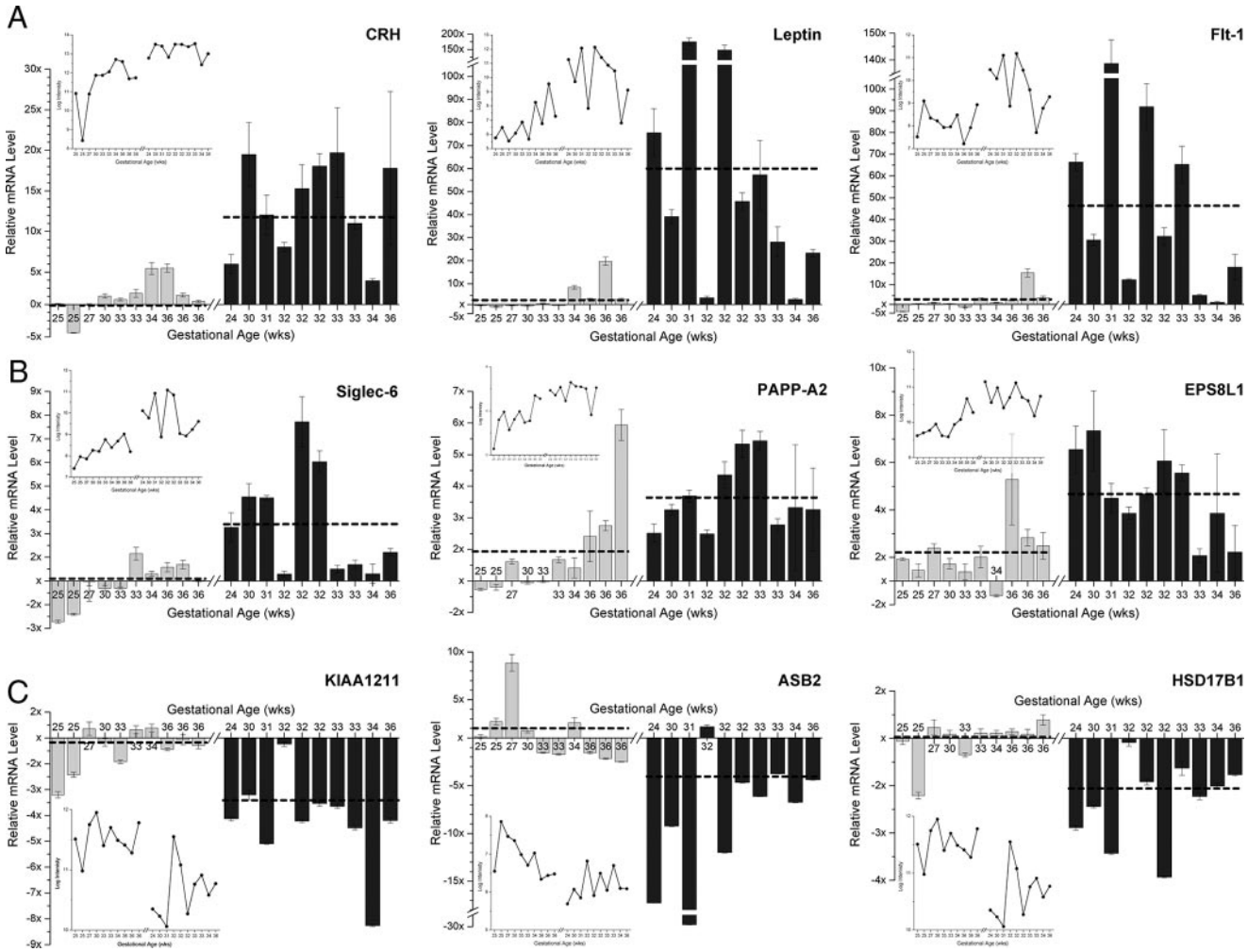

FIG. 3. Q-PCR confirmation of a subset of differentially expressed genes. Total RNA isolated from basal plate biopsies obtained from PTL (24–36 wk; n = 10) or PE (24–36 wk; n = 10) was analyzed using TaqMan primer/probe sets. Relative RNA levels were normalized to 18S values and then divided by a calibrator, in this case a 24-wk PTL sample. Each *bar* represents the mean ± SD of triplicate determinations. PTL, *gray*; PE, *black*. *Dashed lines* are the mean values for the PTL or PE RNAs. Samples are arranged in order of increasing gestational age from *left* to *right* for each category. Significance was determined by using Student's *t* test ($P < 0.05$). For comparison, the *insets* show the corresponding microarray log intensity data for the same samples (log2). A, Q-PCR data for transcripts that were expected to be up-regulated in PE: CRH ($P < 0.0005$), leptin ($P < 0.005$), and Fms-related tyrosine kinase 1 (Flt-1; $P < 0.005$). B, Q-PCR data for novel transcripts up-regulated in PE: Siglec-6 ($P < 0.004$), PAPP-A2 ($P < 0.005$), and epidermal growth factor receptor pathway substrate 8-like protein 1 (EPS8L1; $P < 0.005$). C, Q-PCR data for novel transcripts down-regulated in PE: KIAA1211 protein ($P < 0.005$), ankyrin repeat, SOCS box-containing 2 (ASB2; $P < 0.05$), and hydroxysteroid (17-β) dehydrogenase 1 (HSD17B1; $P < 0.08$).

To identify the cells in the basal plate region that displayed Siglec-6 immunoreactivity, we costained tissue sections from PE (n = 5) and from PTL controls (n = 4) with anti-CK-7, which identifies all subsets of fetal trophoblasts, and with anti-Siglec-6. The results are shown in Fig. 4B. At 24 wk gestation, the PTL tissue exhibited no immunoreactivity. At the same gestational age, STBs and a subset of the maternal cells stained with anti-Siglec-6 in the PE specimens. By 30 wk, the PTL samples showed STB and rare maternal cell staining, reminiscent of the pattern in PE at 24 wk. The fact that Siglec-6 was detected by immunofluorescence at this gestational age and not by immunohistochemistry likely reflects differences in the sensitivity of the methods. In PE tissue at 30 wk, a subset of invasive CTBs also expressed the Siglec-6 antigen. At 36 wk, PTL samples displayed invasive CTB Siglec-6 staining for the first time and continued to have more STB expression. However, the PE sample at 36 wk still showed more Siglec-6 staining overall. This staining pattern may reflect some aspects of premature placental aging or degenerative changes in PE.

We also validated PAPP-A2 expression at the protein level because of its known role in IGF biology, which plays important roles in implantation and placentation. Because antibodies that specifically reacted with PAPP-A2 were not commercially available, we produced a fragment of the PAPP-A2 protein in *E. coli* and used it to immunize rabbits for the purpose of producing polyclonal antibodies. The PAPP-A2 serum, which specifically recognized PAPP-A2, did not cross-react with PAPP-A, the only homolog of PAPP-A2 encoded by the human genome (Fig. 5). In subsequent experiments, we used this antibody for immunoblot analyses, which confirmed increased levels of PAPP-A2 in the PE basal plate compared with PTL (Fig. 6). Densitometry of PAPP-A2 normalized to actin showed roughly a 4.5-fold-higher mean expression in PE compared with PTL (31.35 ± 11.5 *vs.* 7.05 ± 3.53; $P = 0.00001$).

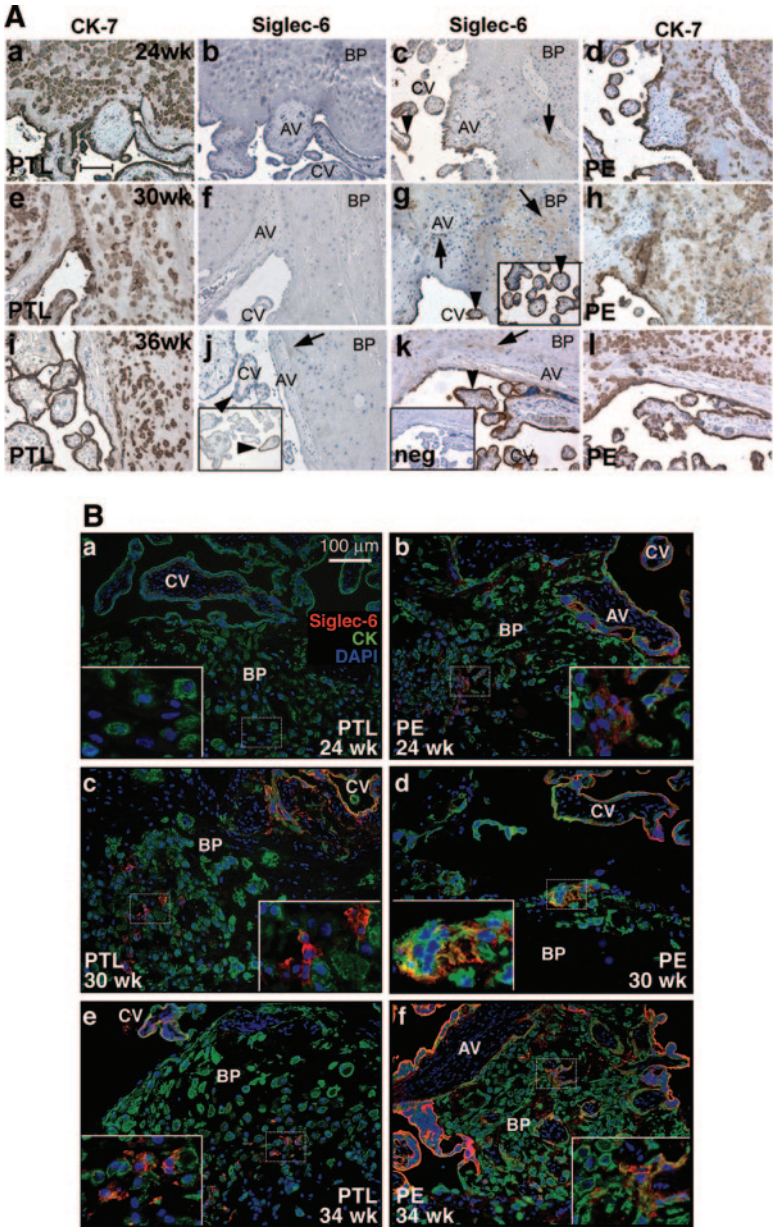

FIG. 4. Siglec-6 expression in basal plate of PE as compared with gestation age-matched, control PTL samples. A, Serial sections of formalin-fixed, paraffin-embedded biopsy specimens of the placental basal plate (BP) region along with floating chorionic villi (CV) and anchoring chorionic villi (AV) from both PTL (n = 11) and PE (n = 14) placentas were stained with anti-CK-7 (1:50), to identify trophoblasts, and anti-Siglec-6 (1:25). Binding was detected with species-specific secondary antibodies and diaminobenzidine. Tissue sections were counterstained with hematoxylin. Photomicrographs are representative of staining patterns of tissues collected at the indicated gestational ages (24–36 wk) after delivery due to PTL (a, b, e, f, i, and j) or PE (c, d, g, h, k, and l). STBs stained for Siglec-6 in all PE samples regardless of gestational age (*arrowheads*: c, g, and k; n = 14). A representative negative control for Siglec-6 staining is shown in the *inset* of k. Before 33 wk, no staining was observed in the PTL samples (b and f; n = 6). At later gestational ages, variable immunoreactivity was observed (j; n = 5). PE samples also showed increased immunoreactivity of cells within the basal plate as compared with PTL controls of the same gestational age (*arrows*). Siglec-6 staining in this region was strongest at 30–32 wk (g; n = 6). *Scale bar*, 100 μm. B, Tissue sections of basal plate biopsy specimens with underlying chorionic villi from PTL (a, c, and e) and PE (b, d, and f) placentas were double stained with anti-CK to identify CTBs (1:50; *green*) and anti-Siglec-6 antibody (1:100, *red*). Binding was detected with the appropriate species-specific secondary antibodies conjugated to fluorescein or rhodamine. Nuclei were labeled with Hoechst (1:1000, *blue*). *Insets* show ×63 magnification of the regions indicated by the *white lines*. Merging of the fluorescein (CK) and rhodamine (Siglec-6) patterns showed that Siglec-6 expression by STBs, maternal cells, and invasive CTBs correlated with gestational age and disease state. Specifically, in PE samples (b, d, and f), Siglec-6 staining was observed at an earlier gestational age and in association with a greater number of cells than in PTL samples (a, c, and e). Photomicrographs are representative of all the samples examined: PTL (n = 4) and PE (n = 5). *Scale bar*, 100 μm.

We used an immunolocalization approach to assess PAPP-A2 expression at the maternal-fetal interface. Serial tissue sections of the human basal plate region from PE (n = 6) and gestational age-matched controls (n = 6) were stained for CK-7 to identify trophoblasts, for HLA-G to identify invasive CTBs, or for PAPP-A2. In both PTL and PE samples, invasive CTBs stained with anti-PAPP-A2. However, at least for the earliest gestational ages, the intensity appeared stronger in the PE samples. For all gestational ages, the PAPP-A2 immunoreactivity of STBs was much more prominent in the PE samples (Fig. 7). Of note, this pattern was distinct from that obtained for PAPP-A expression, which was observed in association with STBs but not invasive CTBs (data not shown).

Discussion

We characterized gene expression profiles at a global level in the basal plate portion of human placentas from pregnancies complicated by preterm PE compared with PTL controls. We were particularly interested in this region because it contains the CTB subpopulations that carry out interstitial and endovascular invasion, the processes that go awry in PE with very dramatic effects associated with the severest forms of this syndrome. Using LOD ratios of B >0, we found that 55 genes were differentially expressed in severe PE. This list included molecules that were previously reported to be present at higher than normal levels in maternal serum, chorionic villi, and/or cord blood in pregnancies complicated by PE, a finding that gives added confidence to the novel genes that we identified as similarly regulated. However, even for these previously reported molecules, in most cases, this is the first description of their increased expression in the basal plate region of the placenta. At the RNA level, we used a Q-PCR approach to confirm the expression patterns of nine of the differentially regulated genes; two of the most interesting novel observations, enhanced Siglec-6 and PAPP-A2 expression, were also validated at the protein level. *In toto*, these results suggest fundamental alterations in important biological processes including pathways that are regulated by leptin and IGF signals.

Other investigators have characterized

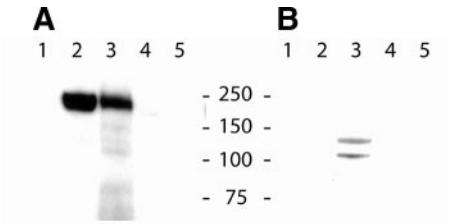

FIG. 5. Immunoblotting showed that the anti-PAPP-A2 polyclonal rabbit antiserum reacted with a single band of the appropriate molecular weight. A, The samples were reduced and separated on a 7% TA Novex gel: lane 1, supernatant from mock-transfected HEK293 cells; lane 2, supernatant from HEK293 cells transfected with PAPP-A2 cDNA; lane 3, term pregnancy serum; lane 4, purified PAPP-A/pro-major basic protein complex; lane 5, supernatant from HEK293 cells transfected with PAPP-A cDNA. The samples were transferred to a PVDF membrane that was incubated overnight with anti-PAPP-A2 (1:10,000). Immunoreactive bands were visualized by incubating the blot with a horseradish peroxidase-conjugated secondary antibody (1:4000) for 1 h at room temperature. A band of about 250 relative molecular mass was detected only in the lanes that contained the recombinant PAPP-A2 protein (lane 2) and pregnancy serum (lane 3). There was no cross-reactivity with the related protein PAPP-A (lanes 4 and 5). B, Identical blot processed the same as in A except incubated with rabbit preimmune serum. Nonspecific bands (~110 and 135 relative molecular mass) were detected in the serum sample (lane 3) only upon overexposure.

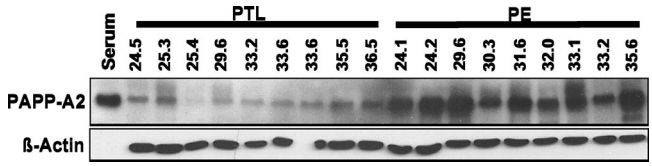

FIG. 6. PAPP-A2 protein levels were increased in the basal plate portion of placentas from PE pregnancies. Protein lysates from basal plate biopsy samples (10 μg) of PTL (n = 9) and PE (n = 9) placentas were separated by SDS-PAGE (4–20% gel). Maternal serum collected at term served as a positive control. Immunoblotting with anti-PAPP-A2 (1:30,000) showed increased immunoreactivity for PAPP-A2 in PE as compared with PTL samples. Immunoblotting with anti-actin (clone C4, 1:10,000) was used as a measure of protein loading. Samples are arranged in order of increasing gestational age from *left* to *right* for each category, with numbers corresponding to gestational age (weeks.days).

(human) placental gene expression patterns in PE compared with normal pregnancy. For example, Reimer *et al.* (45) demonstrated a large increase in leptin production by chorionic villi. A small-scale study with the same design found a PE-associated up-regulation of the gene encoding the muscle subunit of glycogen phosphorylase (46); an increase in the expression of the soluble form of the disintegrin, ADAM 12, was discovered in the same way (47). The fact that we did not identify the latter two molecules is likely attributable to differences in the cellular composition of our samples, which contained a much smaller proportion of chorionic villi and, consequently, STBs that release a myriad of substances into maternal blood. Other relevant considerations include the fact that the causes of PE are complex. For example, in some instances, poor placentation leads to intrauterine growth restriction without PE (7). Conversely, abnormal maternal responses may occur even if placentation is normal (48, 49). In this case, the metabolic, vascular, and immunological demands of pregnancy may synergize with the effects of preexisting medical conditions, such as arterial disease, hypertension, obesity, and diabetes, which in turn strongly predispose women to develop PE. Interestingly, many of these disease processes are associated with altered leptin levels. Numerous investigators have reported a PE-associated increase in circulating levels of leptin (39–44, 50–52), and a leptin gene polymorphism has been linked to an increased risk of developing this pregnancy complication (53). However, a clear picture of how an increase in leptin expression is linked to the pathophysiology of PE has yet to emerge.

Our data demonstrated increased leptin expression in the basal plate of PE placentas compared with control tissue. Interestingly, although the classic leptin receptors were not differentially expressed, we observed elevated levels of the mRNA that encodes Siglec-6, a transmembrane protein that also binds leptin. These findings suggest that this molecule may play an important role as a placental leptin receptor and that increased Siglec-6 levels could contribute to the pathogenesis of PE. Although the cloning strategy for Siglec-6 was based on its ability to interact with leptin, the other Siglec family members bind sialic acid-containing glycans. Some family members have exquisite ligand specificity, whereas others have less rigid structural requirements (54). For example, Siglec-6 has binding specificity for the sialyl-Tn epitope (Siaα2–6Gal-NAcα1-O-R, where R is a serine or threonine). Published data suggest that in the placenta, leptin is a Siglec-6 ligand, but the endogenous binding partners have yet to be identified (26). Additionally, Siglec-6 expression has other interesting features. For example, in humans, it is restricted to the placenta and B lymphocytes. In other species, including nonhuman primates, placental cells lack Siglec-6 expression, whereas the B cells exhibit it (25). The fact that Siglec-6 is expressed only in human placentas and not in nonhuman primate placentas (25) is extremely intriguing, because PE is thought to be a uniquely human disease; spontaneous PE has not been reported in other animals, even nonhuman primates (55).

The function(s) of Siglec-6 in any biological system, including B cells, have yet to be determined. A recent study suggested a role for Siglec-6 in term labor (25). Interestingly, Siglec-6 expression was not observed in our earliest gestation PTL samples but did increase as pregnancy advanced. Siglec-6 has conserved immunoreceptor tyrosine-based inhibitory motif (ITIM) and ITIM-like domains, suggesting that ligand binding results in tyrosine phosphorylation and recruitment of Src homology domain-containing adapters with inhibitory effects. The effect of leptin has been investigated in mice and bats (56, 57). In both species, leptin appears to have a stimulatory effect on trophoblast invasion *in vitro*, but its mechanism of action is not known. Determining whether leptin and Siglec-6 function during human CTB invasion is a critical first step in understanding whether these molecules play a functional role in PE pathogenesis.

A PE-associated increase in the expression of PAPP-A2 was another novel observation that emerged from our work. This is the first report of PAPP-A2 expression at the protein level in the placenta, experiments that were made possible by the generation of rabbit polyclonal antibodies that specifically reacted with this molecule. PAPP-A2, which has 46% sequence identity with PAPP-A, is a metalloproteinase that cleaves IGF-binding protein-5 (IGFBP-5) (28). Depending on the cellular context, IGFBPs either stimulate or inhibit IGF-I and -II actions. For example, in smooth muscle cells, IGFBP-5 binds to extracellular matrix com-

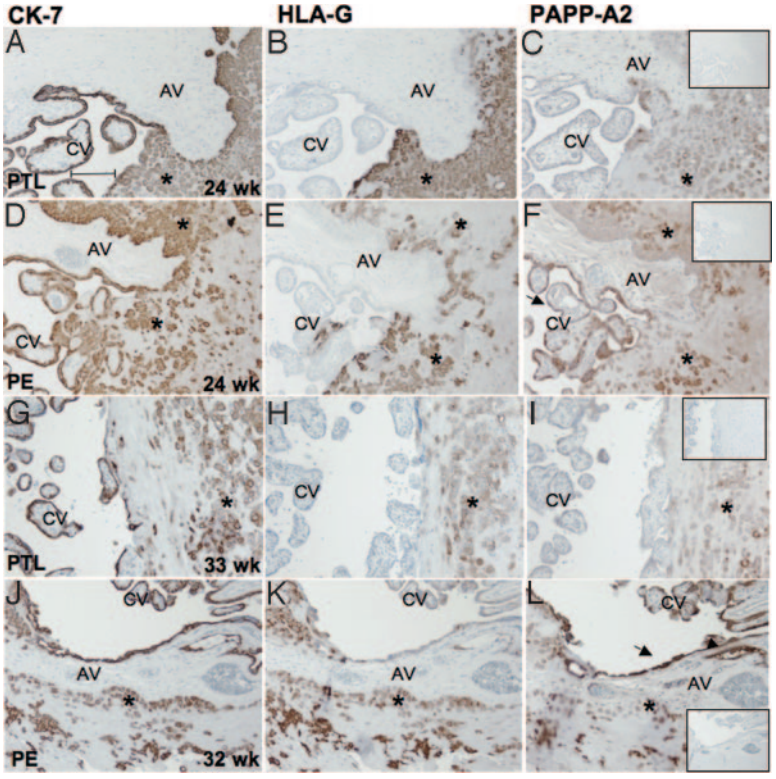

FIG. 7. PE is associated with enhanced staining of invasive CTBs and STBs for PAPP-A2. Serial sections of formalin-fixed, paraffin-embedded basal plate biopsy specimens of placentas from PTL (A–C and G–I) and PE (D–F and J–L) at various gestational ages were stained with anti-CK-7 (1:100) to identify trophoblasts, anti-HLA-G (1:50) to identify invasive CTBs, or anti-PAPP-A2 (1:30,000). Binding of the primary antibody was detected with the appropriate species-specific secondary antibody and diaminobenzidine. Tissue sections were counterstained with hematoxylin. Invasive CTBs (*) reacted with anti-PAPP-A2 in all the samples, but the staining intensity (when using HLA-G and CK-7 levels for comparison) was greater in PE at the earlier gestational ages than in PTL. In contrast, PAPP-A2 immunoreactivity of STB, which was a prominent feature of PE samples (F and L, *arrows*), was largely absent in PTL specimens (C and I). Negative controls for PAPP-A2 staining are shown as *insets* (C, F, I, and L). Photomicrographs are representative of multiple analyses (PTL, n = 6; PE, n = 6). AV, Anchoring chorionic villi; CV, floating chorionic villi. *Scale bar*, 200 μm.

ponents, including thrombospondin-1 and osteopontin, and potentiates the cells' response to IGF-I. In contrast, IGFBP-4, a PAPP-A substrate, largely inhibits IGF actions (58). In a fibroblast model, an increase in IGFBP-5 proteolysis attenuates its stimulatory effects on cell migration (59). If CTBs respond in an analogous manner, then the observed PE-associated increase in PAPP-A2 levels could inhibit CTB invasion by mechanisms that include an increase in IGFBP-5 proteolysis.

Data suggest that there is cross talk between the (classical) leptin and insulin signaling pathways (60). Specifically, suppressor of cytokine signaling (SOCS-3) attenuates both pathways (61). Furthermore, related Siglec family members' (CD33/Siglec-3 and Siglec-7) responses are blocked by SOCS-3 via accelerated proteasomal degradation (62, 63). Given that IGF and insulin signal through the same pathways, it is possible that alterations in leptin, Siglec-6, and PAPP-A2 levels may be working in concert to exert inhibitory effects on CTB invasion. Understanding the pregnancy-related functions of these molecules and the other genes that were differentially expressed in PE will likely lead to a better understanding of the pathogenesis of this human-specific condition, the crucial first step in the rational design of treatments (both preventative and therapeutic) that address the causes, rather than the consequences, of this pregnancy complication. Additionally, we envision that PE-associated alterations in the expression of gene products that are secreted in maternal blood can be used to predict a woman's risk of developing this syndrome and/or enable diagnosis during the early stages of PE when the signs are sometimes ambiguous.

Acknowledgments

We thank Ms. Jean Perry, the study research nurse coordinator, who assisted in tissue collection, as did the nurses, residents, and faculty at the UCSF Birth Center. Dr. Chris Barker, Dr. Chandi Griffin, and Ms. Jennifer Gregg, members of the UCSF Gladstone (National Heart, Lung, and Blood Institute) Shared Microarray Facility, contributed invaluable technical and intellectual expertise. We also thank Dr. David Erle and Michael Salazar, members of the Sandler Genomics Core Facility, and Nissi Varki (University of California, San Diego) for helpful discussions. We are grateful to Mr. Evan Messenger and Dr. Kathy Ivanetich, UCSF Biomolecular Research Center, for technical assistance in performing the Q-PCR experiments. We thank Ms. Mary McKenney for critical review of the manuscript.

Address all correspondence and requests for reprints to: Virginia D. Winn, M.D., Ph.D., University of Colorado Denver, Department of Obstetrics and Gynecology, Reproductive Sciences, Mail Stop 8309, 12800 East 19th Avenue, P.O. Box 6511, Aurora, Colorado 80045. E-mail: Virginia.Winn@ucdenver.edu.

This work was supported by National Institutes of Health Grants R01 HL 64597 (to S.J.F.), R01 GM 32373 (to A.V.), 5-MO1-RR 00083 (General Clinical Research Center, San Francisco General Hospital), HL 072301 (UCSF, National Heart, Lung, and Blood Institute Shared Microarray Facility), and the Danish Medical Research Council (to C.O.). V.D.W. is a March of Dimes Reproductive Scientists Development Program scholar (National Institute of Child Health and Human Development 5K12HD00849) and an American Board of Obstetrics and Gynecology/American Association of Obstetricians and Gynecologists Foundation scholar.

Disclosure Statement: M.G., A.G., K.K.-S., A.K., K.R., R.-F.Y., M.T.O., and A.V. have nothing to declare. V.D.W., R.H.-K., and S.J.F. have a patent filed for the array data. V.D.W., C.O., and S.J.F. have research grants as listed above.

References

1. **Roberts JM, Cooper DW** 2001 Pathogenesis and genetics of pre-eclampsia. Lancet 357:53–56
2. **Gomez O, Martinez JM, Figueras F, Del Rio M, Borobio V, Puerto B, Coll O, Cararach V, Vanrell JA** 2005 Uterine artery Doppler at 11–14 weeks of gestation to screen for hypertensive disorders and associated complications in an unselected population. Ultrasound Obstet Gynecol 26:490–494
3. **Hershkovitz R, de Swiet M, Kingdom J** 2005 Mid-trimester placentation assessment in high-risk pregnancies using maternal serum screening and uterine artery Doppler. Hypertens Pregnancy 24:273–280

4. **Brosens IA, Robertson WB, Dixon HG** 1972 The role of the spiral arteries in the pathogenesis of preeclampsia. Obstet Gynecol Annu 1:177–191
5. **Gerretsen G, Huisjes HJ, Elema JD** 1981 Morphological changes of the spiral arteries in the placental bed in relation to pre-eclampsia and fetal growth retardation. Br J Obstet Gynaecol 88:876–881
6. **Moodley J, Ramsaroop R** 1989 Placental bed morphology in black women with eclampsia. S Afr Med J 75:376–378
7. **Khong TY, De Wolf F, Robertson WB, Brosens I** 1986 Inadequate maternal vascular response to placentation in pregnancies complicated by pre-eclampsia and by small-for-gestational age infants. Br J Obstet Gynaecol 93:1049–1059
8. **Roberts JM, Taylor RN, Musci TJ, Rodgers GM, Hubel CA, McLaughlin MK** 1989 Preeclampsia: an endothelial cell disorder. Am J Obstet Gynecol 161: 1200–1204
9. **Roberts JM** 1998 Endothelial dysfunction in preeclampsia. Semin Reprod Endocrinol 16:5–15
10. **Friedman SA, Schiff E, Emeis JJ, Dekker GA, Sibai BM** 1995 Biochemical corroboration of endothelial involvement in severe preeclampsia. Am J Obstet Gynecol 172:202–203
11. **Hsu CD, Iriye B, Johnson TR, Witter FR, Hong SF, Chan DW** 1993 Elevated circulating thrombomodulin in severe preeclampsia. Am J Obstet Gynecol 169:148–149
12. **Taylor RN, Crombleholme WR, Friedman SA, Jones LA, Casal DC, Roberts JM** 1991 High plasma cellular fibronectin levels correlate with biochemical and clinical features of preeclampsia but cannot be attributed to hypertension alone. Am J Obstet Gynecol 165:895–901
13. **Tyurin VA, Liu SX, Tyurina YY, Sussman NB, Hubel CA, Roberts JM, Taylor RN, Kagan VE** 2001 Elevated levels of S-nitrosoalbumin in preeclampsia plasma. Circ Res 88:1210–1215
14. **Clark BA, Halvorson L, Sachs B, Epstein FH** 1992 Plasma endothelin levels in preeclampsia: elevation and correlation with uric acid levels and renal impairment. Am J Obstet Gynecol 166:962–968
15. **Mills JL, DerSimonian R, Raymond E, Morrow JD, Roberts 2nd LJ, Clemens JD, Hauth JC, Catalano P, Sibai B, Curet LB, Levine RJ** 1999 Prostacyclin and thromboxane changes predating clinical onset of preeclampsia: a multicenter prospective study. JAMA 282:356–362
16. **Levine RJ, Lam C, Qian C, Yu KF, Maynard SE, Sachs BP, Sibai BM, Epstein FH, Romero R, Thadhani R, Karumanchi SA** 2006 Soluble endoglin and other circulating antiangiogenic factors in preeclampsia. N Engl J Med 355:992–1005
17. **Winn VD, Haimov-Kochman R, Paquet AC, Yang YJ, Madhusudhan MS, Gormley M, Feng KT, Bernlohr DA, McDonagh S, Pereira L, Sali A, Fisher SJ** 2007 Gene expression profiling of the human maternal-fetal interface reveals dramatic changes between midgestation and term. Endocrinology 148:1059–1079
18. **Zhou Y, Bianco K, Huang L, Nien JK, McMaster M, Romero R, Fisher SJ** 2007 Comparative analysis of the maternal-fetal interface in preeclampsia and preterm labor. Cell Tissue Res 329:559–569
19. **American College of Obstetricians and Gynecologists** 1999 Practice bulletin 10. Induction of labor. Washington, DC: American College of Obstetricians and Gynecologists
20. **Haimov-Kochman R, Fisher SJ, Winn VD** 2006 Modification of the standard Trizol-based technique improves the integrity of RNA isolated from RNase-rich placental tissue. Clin Chem 52:159–160
21. **Auer H, Lyianarachchi S, Newsom D, Klisovic MI, Marcucci G, Kornacker K** 2003 Chipping away at the chip bias: RNA degradation in microarray analysis. Nat Genet 35:292–293
22. **Gentleman RC, Carey VJ, Bates DM, Bolstad B, Dettling M, Dudoit S, Ellis B, Gautier L, Ge Y, Gentry J, Hornik K, Hothorn T, Huber W, Iacus S, Irizarry R, Leisch F, Li C, Maechler M, Rossini AJ, Sawitzki G, Smith C, Smyth G, Tierney L, Yang JY, Zhang J** 2004 Bioconductor: open software development for computational biology and bioinformatics. Genome Biol 5:R80
23. **Bolstad BM** 2004 Low level analysis of high-density oligonucleotide array data: background, normalization and summarization. Dissertation, University of California, Berkeley
24. **Smyth GK** 2005 Limma: linear models for microarray data. In: Gentleman R, Carey V, Huber W, Irizarry R, Dudoit S, eds. Bioinformatics and computational biology solutions Using R and Bioconductor. New York: Springer; 397–420
25. **Brinkman-Van der Linden EC, Hurtado-Ziola N, Hayakawa T, Wiggleton L, Benirschke K, Varki A, Varki N** 2007 Human-specific expression of Siglec-6 in the placenta. Glycobiology 17:922–931
26. **Patel N, Brinkman-Van der Linden EC, Altmann SW, Gish K, Balasubramanian S, Timans JC, Peterson D, Bell MP, Bazan JF, Varki A, Kastelein RA** 1999 OB-BP1/Siglec-6: a leptin- and sialic acid-binding protein of the immunoglobulin superfamily. J Biol Chem 274:22729–22738
27. **Damsky CH, Fitzgerald ML, Fisher SJ** 1992 Distribution patterns of extracellular matrix components and adhesion receptors are intricately modulated during first trimester cytotrophoblast differentiation along the invasive pathway, in vivo. J Clin Invest 89:210–222
28. **Overgaard MT, Boldt HB, Laursen LS, Sottrup-Jensen L, Conover CA, Oxvig C** 2001 Pregnancy-associated plasma protein-A2 (PAPP-A2), a novel insulin-like growth factor-binding protein-5 proteinase. J Biol Chem 276:21849–21853
29. **Ellgaard L, Holtet TL, Nielsen PR, Etzerodt M, Gliemann J, Thogersen HC** 1997 Dissection of the domain architecture of the α2macroglobulin-receptor-associated protein. Eur J Biochem 244:544–551
30. **Anderson M, Blowers D, Hewitt N, Hedge P, Breeze A, Hampton I, Taylor I** 1999 Refolding, purification, and characterization of a loop deletion mutant of human Bcl-2 from bacterial inclusion bodies. Protein Expr Purif 15:162–170
31. **Harlow E. LD** 1988 Antibodies: a laboratory manual. Cold Spring Harbor, NY: Cold Spring Harbor Laboratory Press
32. **Oxvig C, Sand O, Kristensen T, Kristensen L, Sottrup-Jensen L** 1994 Isolation and characterization of circulating complex between human pregnancy-associated plasma protein-A and proform of eosinophil major basic protein. Biochim Biophys Acta 1201:415–423
33. **Overgaard MT, Haaning J, Boldt HB, Olsen IM, Laursen LS, Christiansen M, Gleich GJ, Sottrup-Jensen L, Conover CA, Oxvig C** 2000 Expression of recombinant human pregnancy-associated plasma protein-A and identification of the proform of eosinophil major basic protein as its physiological inhibitor. J Biol Chem 275:31128–31133
34. **Qin QP, Christiansen M, Oxvig C, Pettersson K, Sottrup-Jensen L, Koch C, Norgaard-Pedersen B** 1997 Double-monoclonal immunofluorometric assays for pregnancy-associated plasma protein A/proeosinophil major basic protein (PAPP-A/proMBP) complex in first-trimester maternal serum screening for Down syndrome. Clin Chem 43:2323–2332
35. **McMaster MT, Librach CL, Zhou Y, Lim KH, Janatpour MJ, DeMars R, Kovats S, Damsky C, Fisher SJ** 1995 Human placental HLA-G expression is restricted to differentiated cytotrophoblasts. J Immunol 154:3771–3778
36. **American College of Obstetrics and Gynecology** 2002 ACOG Practice Bulletin: diagnosis and management of preeclampsia and eclampsia. Obstet Gynecol 99:159–167
37. **Muttukrishna S, Knight PG, Groome NP, Redman CW, Ledger WL** 1997 Activin A and inhibin A as possible endocrine markers for pre-eclampsia. Lancet 349:1285–1288
38. **Perkins AV, Linton EA, Eben F, Simpson J, Wolfe CD, Redman CW** 1995 Corticotrophin-releasing hormone and corticotrophin-releasing hormone binding protein in normal and pre-eclamptic human pregnancies. Br J Obstet Gynaecol 102:118–122
39. **Laivuori H, Gallaher MJ, Collura L, Crombleholme WR, Markovic N, Rajakumar A, Hubel CA, Roberts JM, Powers RW** 2006 Relationships between maternal plasma leptin, placental leptin mRNA and protein in normal pregnancy, pre-eclampsia and intrauterine growth restriction without pre-eclampsia. Mol Hum Reprod 12:551–556
40. **Li RH, Poon SC, Yu MY, Wong YF** 2004 Expression of placental leptin and leptin receptors in preeclampsia. Int J Gynecol Pathol 23:378–385
41. **Lu D, Yang X, Wu Y, Wang H, Huang H, Dong M** 2006 Serum adiponectin, leptin and soluble leptin receptor in pre-eclampsia. Int J Gynaecol Obstet 95:121–126
42. **McCarthy JF, Misra DN, Roberts JM** 1999 Maternal plasma leptin is increased in preeclampsia and positively correlates with fetal cord concentration. Am J Obstet Gynecol 180:731–736
43. **Tommaselli GA, Pighetti M, Nasti A, D'Elia A, Guida M, Di Carlo C, Bifulco G, Nappi C** 2004 Serum leptin levels and uterine Doppler flow velocimetry at 20 weeks' gestation as markers for the development of pre-eclampsia. Gynecol Endocrinol 19:160–165
44. **Vitoratos N, Chrystodoulacos G, Kouskouni E, Salamalekis E, Creatsas G** 2001 Alterations of maternal and fetal leptin concentrations in hypertensive disorders of pregnancy. Eur J Obstet Gynecol Reprod Biol 96:59–62
45. **Reimer T, Koczan D, Gerber B, Richter D, Thiesen HJ, Friese K** 2002 Microarray analysis of differentially expressed genes in placental tissue of pre-eclampsia: up-regulation of obesity-related genes. Mol Hum Reprod 8:674–680
46. **Tsoi SC, Cale JM, Bird IM, Kay HH** 2003 cDNA microarray analysis of gene expression profiles in human placenta: up-regulation of the transcript encoding muscle subunit of glycogen phosphorylase in preeclampsia. J Soc Gynecol Investig 10:496–502
47. **Gack S, Marme A, Marme F, Wrobel G, Vonderstrass B, Bastert G, Lichter P, Angel P, Schorpp-Kistner M** 2005 Preeclampsia: increased expression of soluble ADAM 12. J Mol Med 83:887–896

48. **Ness RB, Roberts JM** 1996 Heterogeneous causes constituting the single syndrome of preeclampsia: a hypothesis and its implications. Am J Obstet Gynecol 175:1365–1370
49. **Redman CW, Sargent IL** 2005 Latest advances in understanding preeclampsia. Science 308:1592–1594
50. **Laivuori H, Kaaja R, Koistinen H, Karonen SL, Andersson S, Koivisto V, Ylikorkala O** 2000 Leptin during and after preeclamptic or normal pregnancy: its relation to serum insulin and insulin sensitivity. Metabolism 49:259–263
51. **Mise H, Sagawa N, Matsumoto T, Yura S, Nanno H, Itoh H, Mori T, Masuzaki H, Hosoda K, Ogawa Y, Nakao K** 1998 Augmented placental production of leptin in preeclampsia: possible involvement of placental hypoxia. J Clin Endocrinol Metab 83:3225–3229
52. **Ramsay JE, Ferrell WR, Crawford L, Wallace AM, Greer IA, Sattar N** 2004 Divergent metabolic and vascular phenotypes in pre-eclampsia and intrauterine growth restriction: relevance of adiposity. J Hypertens 22:2177–2183
53. **Muy-Rivera M, Ning Y, Frederic IO, Vadachkoria S, Luthy DA, Williams MA** 2005 Leptin, soluble leptin receptor and leptin gene polymorphism in relation to preeclampsia risk. Physiol Res 54:167–174
54. **Varki A, Angata T** 2006 Siglecs: the major subfamily of I-type lectins. Glycobiology 16:1R–27R
55. **Chez RA** 1976 Nonhuman primate models of toxemia of pregnancy. Perspect Nephrol Hypertens 5:421–424
56. **Schulz LC, Townsend K, Kunz TH, Widmaier EP** 2007 Inhibition of trophoblast invasiveness in vitro by immunoneutralization of leptin in the bat, *Myotis lucifugus* (*Chiroptera*). Gen Comp Endocrinol 150:59–65
57. **Schulz LC, Widmaier EP** 2004 The effect of leptin on mouse trophoblast cell invasion. Biol Reprod 71:1963–1967
58. **Firth SM, Baxter RC** 2002 Cellular actions of the insulin-like growth factor binding proteins. Endocr Rev 23:824–854
59. **Xu Q, Yan B, Li S, Duan C** 2004 Fibronectin binds insulin-like growth factor-binding protein 5 and abolishes its ligand-dependent action on cell migration. J Biol Chem 279:4269–4277
60. **Fruhbeck G** 2006 Intracellular signalling pathways activated by leptin. Biochem J 393:7–20
61. **Howard JK, Flier JS** 2006 Attenuation of leptin and insulin signaling by SOCS proteins. Trends Endocrinol Metab 17:365–371
62. **Orr SJ, Morgan NM, Buick RJ, Boyd CR, Elliott J, Burrows JF, Jefferies CA, Crocker PR, Johnston JA** 2007 SOCS3 targets Siglec 7 for proteasomal degradation and blocks Siglec 7-mediated responses. J Biol Chem 282:3418–3422
63. **Orr SJ, Morgan NM, Elliott J, Burrows JF, Scott CJ, McVicar DW, Johnston JA** 2007 CD33 responses are blocked by SOCS3 through accelerated proteasomal-mediated turnover. Blood 109:1061–1068